Power Measurement Errors on a Utility Aircraft

WILLIAM G. BOUSMAN

Army/NASA Rotorcraft Division
Aeroflightdynamics Directorate (AMRDEC)
US Army Aviation and Missile Command
Ames Research Center, Moffett Field, California

Abstract

Extensive flight test data obtained from two recent performance tests of a UH–60A aircraft are reviewed. A power difference is calculated from the power balance equation and is used to examine power measurement errors. It is shown that the baseline measurement errors are highly non-Gaussian in their frequency distribution and are therefore influenced by additional, unquantified variables. Linear regression is used to examine the influence of other variables and it is shown that a substantial portion of the variance depends upon measurements of atmospheric parameters. Correcting for temperature dependence, although reducing the variance in the measurement errors, still leaves unquantified effects. Examination of the power difference over individual test runs indicates significant errors from drift, although it is unclear how these may be corrected. In an idealized case, where the drift is correctable, it is shown that the power measurement errors are significantly reduced and the error distribution is Gaussian. A new flight test program is recommended that will quantify the thermal environment for all torque measurements on the UH–60. Subsequently, the torque measurement systems will be recalibrated based on the measured thermal environment and a new power measurement assessment performed.

Notation

A	rotor disk area, ft^2
C_P	power coefficient, $P/\rho A V_T^3$
C_T	thrust coefficient, $GW/\rho A V_T^2$
GW	gross weight, lb
H_p	pressure altitude, ft
N_{run}	run number
n	number of test points
P	power, HP
r^2	coefficient of determination
SHP_a	accessory power, HP
SHP_e	combined engine power, HP
SHP_r	main rotor power, HP
SHP_{tr}	tail rotor drive shaft power, HP
T	outside air temperature, deg C
V_T	rotor tip speed, ft/sec
ΔP	power difference, eq. (5), HP
ΔP_T	power difference corrected for temperature, eq. (6), HP
ΔP_{Td}	power difference corrected for temperature and drift, eq. (7), HP
ε	measurement errors, HP
η	main gear box efficiency, 0.98389
ρ	density of air, slugs/ft^3
σ	standard deviation

Presented at the American Helicopter Society Aerodynamics, Acoustics, and Test and Evaluation Technical Specialists Meeting, San Francisco, CA, January 23-25, 2002.

Introduction

The accurate knowledge of performance in hover and forward flight is a key requirement for any helicopter. However, performance measurements are difficult to make if accuracies of the order of 1 to 2% are desired. Each of the significant variables that influence performance, that is power required, rotor thrust, and aircraft velocity, have their own unique measurement problems. The measurement of power requires a highly accurate torquemeter for the engine output and this accuracy must be sustained under high loading conditions and in a hot environment. Rotor thrust (and propulsive force) depends not only on the vehicle weight, but also on the lift from the fuselage and the horizontal tailplane, download on the fuselage from the rotor induced flow, and, in the case of an aircraft such as the UH–60, on the lift from the canted tail rotor. The measurement of aircraft velocity in forward flight requires an accurately calibrated airspeed system, while in hover it is essential to demonstrate that the relative wind velocity is near zero.

The UH–60 is the U.S. Army's primary troop carrying transport. Since its initial procurement in 1977, the hover and forward flight performance of this aircraft have been measured on repeated occasions (Refs. 1–8). For these test programs, the power required has been obtained using calibrated torquemeters on the output shafts of both engines. In addition, the main rotor shaft torque and tail rotor drive shaft torque have also been measured. Rotor thrust has not been measured, but instead has been assumed to be the same as the aircraft's gross weight. During tests, the initial aircraft gross weight is accurately known and fuel totalizers are used during a flight to define the gross weight on a continuous basis. Hover performance testing has generally been done using a tether system with data obtained only for winds less than three knots. Forward flight performance testing requires an accurate airspeed calibration.

Using these measurement approaches and normal flight test practice, there has been the general expectation that measured performance data will follow theoretical considerations. As an example, in hover, it is expected that nondimensionalized test data will fall on a single curve defined by

$$C_P = C_T^{1.5} \tag{1}$$

However, this relationship is only approximate, as C_P for these tests is based on the engine output power, not rotor power, and C_T is based on gross weight and neglects the download on the fuselage from the rotor induced flow and the lift from the canted tail rotor. For the UH–60, the engine output power is roughly proportional to the main rotor power. For example, in the testing reported in Ref. 8, if the main rotor power measurement is normalized to 1.00, then the engine output power is 1.19, or 19% higher, with a normalized standard deviation of ±0.07 (n = 763). The download is unmeasured, but based on the model experiments reported in Ref. 9, this download is approximately 4.5% of rotor thrust at low thrust values, dropping to about 3.0% of rotor thrust at high values. The lift from the canted tail rotor contributes about 2.7% of the total aircraft thrust and is proportional to main rotor torque. To accommodate these approximations, eq. (1) is normally expressed as

$$C_P = A_0 + A_1 C_T^{1.5} \tag{2}$$

where A_0 is normally very small and A_1 is close to unity.

Unfortunately, the nondimensionalization of eq. (2) has not always been satisfactory. In Ref. 1, tethered hover testing was performed at three different elevations, ranging from 2302 feet at Edwards AFB, California, to 9980 feet at Coyote Flats, California. The test report noted that the data sets from each elevation were best fit by separate curves, that is, they were density altitude dependent. The report recommended that the handbook performance calculations be based on a variant of eq. (2)

$$C_P = A_0 + A_1 C_T^{1.5} + \Delta C_P \tag{3}$$

where ΔC_P was provided graphically, based on the density altitude.

Hover testing of a sixth-year production aircraft (Ref. 3) was also performed at three different elevations. However, in this case, a good match of the data was obtained if eq. (2) was modified to include a higher-order term

$$C_P = A_0 + A_1 C_T^{1.5} + A_2 C_T^{3} \tag{4}$$

The data from Ref. 1 were reanalyzed in the same way and it was shown that about three percent more power was required for OGE hover with the sixth-year aircraft. The increased power was ascribed to the addition of fairings for the Extended Stores Support System (ESSS), see also Ref. 2. Attempts were made in Ref. 3 to match the forward flight performance of the first- and sixth-year production aircraft and these were not completely successful, even after correcting for flat plate drag increases. About half of the discrepancy could be explained based on the dimensional schedule of the stabilator angle of attack, but the remaining power difference could not be accounted for.

NASA and the U.S. Army undertook a set of detailed flight test measurements on a highly-instrumented UH–60A in the early 1990s under the NASA/Army UH–60A Airloads Program (Ref. 7). Although the focus of this test program was on measured blade pressures, performance testing was also accomplished using the same measurement approach as in previous UH–60A performance tests. These performance measurements have been examined for their internal consistency and substantial discrepancies in the measurement of power have been observed (Ref. 10). In this study the power train measurements were formulated into a power balance equation

$$\Delta P = SHP_a + \varepsilon = SHP_e - \frac{1}{\eta}(SHP_r + SHP_{tr}) \qquad (5)$$

where all measured powers were grouped on the right hand side and the unmeasured accessory power and power measurement errors were grouped on the left hand side. The accessory power was estimated to be 66 HP (Ref. 8) and, except for the oil cooler fan, should not vary during testing. For this test program, ΔP ranged from –40 to 175 HP, which, if compared to the power required to hover for the primary mission, equates to measurement errors of ±5.3%.

New rotor blades for the UH–60 fleet have been in development over the last decade. Prototype blades with new airfoils and an increased chord, referred to as the Wide Chord Blades (WCB), were tested on a UH–60L aircraft with –701C engines from March to November 1999 (Ref. 8). This testing was performed by a combined Sikorsky/Army test team at West Palm Beach, Florida, and Alamosa, Colorado. Performance data were obtained in hover and forward flight. The hover data obtained in Florida and Colorado were not consistent and it was noted that there were “uncertainties relative to engine torquemeter calibration, unexpected data trends (including reverse compressibility effects and conflicting whirlstand data trends).”

It is unclear whether all of the various problems observed in performance testing of the UH–60 are related. However, performance data obtained in two of these tests (Refs. 7 and 8) are sufficiently detailed that the power balance equation can be used to examine the nature of the power measurement errors and that is the purpose of the present paper. In the sections below, the two databases that are used will be described. The power measurement errors for the data will be examined and their basic form characterized. The dependency of the measurement errors on other variables will be examined using linear regression. It will be shown that the outside air temperature influences the power measurement errors and the effects of temperature corrections on the measurement errors will be shown. The effects of drift of the measurements will also be examined and an idealized case will be defined to show the improvement in accuracy that can be obtained if errors caused by drift can be corrected. Conclusions will be provided from the analysis presented here as well as recommendations for a program of flight tests and transducer calibration to resolve the temperature-induced power measurement errors.

Data Sets

UH–60A Airloads Program

Highly-instrumented rotor blades were built for a UH–60A and were installed on a UH–60A aircraft which was tested at the NASA Ames Research Center under a joint NASA–Army program (Ref. 7). Thirty-one research flights were conducted from July 1993 to February 1994, and approximately 58 flight test hours were flown. The aircraft used for this program was a sixth-year production aircraft, S/N 82-23748, that had been updated to meet U.S. Army fleet requirements. The data from this program are in an electronic database at Ames Research Center and are accessible to qualified researchers.

Only limited hover test data were obtained during the Airloads Program and these data are not comparable to hover performance data from either earlier or later flight test programs. However, forward flight performance testing was accomplished for six weight coefficients and these data are comparable to the other UH–60 data examined here. This data set is comprised of 103 test points or counters, for pressure altitudes from sea level to 17,000 feet, and advance ratios from zero to 0.368.

A schematic of the power train layout on the UH–60 is shown in Fig. 1. The power balance, eq. (5), is taken at the input to the main gearbox. The main gearbox efficiency, η, is 0.98389. Power measurements were obtained on the engine output shafts of both engines, SHP_{e1} and SHP_{e2}, on the main rotor shaft, SHP_r, and on the tail rotor output drive shaft, SHP_{tr}. The accessory power, SHP_a, was not measured. The engine power was calculated from the engine output shaft torque, which was measured using a torque sleeve or tube that surrounded the output drive shaft, but was only pinned at one end. The relative twist between the output drive shaft and the unloaded torque sleeve then provided a measure of the engine torque. To measure the relative twist, two teeth were mounted on the outer surface of the output drive shaft, 180 deg apart, and a second set of two teeth were mounted on the inner surface of the torque sleeve, offset by 90 deg from the drive shaft teeth. A magnetic sensor

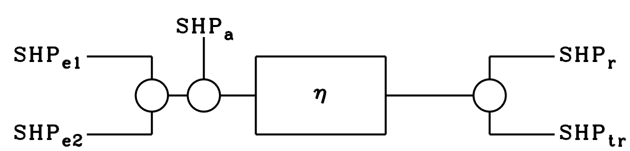

Figure 1. – Schematic of UH–60A power train; power balance taken at input to the main gearbox.

in the fixed system was used to generate a signal based on the passage of the four teeth and in this way determine the twist angle between the inner shaft and outer sleeve. The processing algorithm also used the exhaust gas temperature to correct the torque measurement for temperature effects. The engine torquemeters were calibrated in a test cell by General Electric, the engine manufacturer.

Main rotor power was based on the measurement of the main rotor torque using a strain-gauge bridge mounted on the main rotor mast. This strain-gauge bridge was calibrated by Sikorsky Aircraft in a special-purpose calibration rig. The tail rotor output drive shaft from the main gearbox was instrumented with two strain-gauge bridges to measure shaft torque. Both bridges were mounted on the tail rotor drive shaft just before the intermediate tail rotor gearbox at the base of the tail. These bridges were calibrated by loading the drive shaft with known torques.

The test aircraft was weighed periodically during the test program, although not before every flight. A normal weight and balance was computed for every flight and the fuel load was measured. Fuel burnoff during the flight was measured and the aircraft actual weight was computed for all test points.

Wide Chord Blade Test Program

Sikorsky Aircraft and the U.S. Army have worked on the development of a new set of rotor blades for the UH–60 to provide better performance at high gross weights. The new blade design has been variously referred to as the Growth Rotor Blade (GRB) or Wide Chord Blade (WCB). The latter nomenclature is used here as the test data in Ref. 8 were obtained with a prototype set of blades that are slightly different from the GRB set that will go on the UH–60M aircraft.

Under the WCB development and qualification program, flight testing was accomplished on two aircraft, a UH–60L, S/N 84-23953 and a MH-60K, S/N 91-26387. The flight program totaled approximately 125 flight hours of which 111 hours were flown at Sikorsky Aircraft's Flight Development Facility at West Palm Beach, Florida, and 14 hours were flown at a high-altitude test site at Alamosa, Colorado. Eighteen of the 125 flight hours were used for performance testing and all of these tests were flown with aircraft 953, the UH–60L.

Extensive IGE and OGE hover test data were obtained, with most of the points using a tethered hover test technique. Hover testing was performed at both the Florida and Colorado sites, with pressure altitudes of sea level and about 7,100 feet. Hover gross weights varied from 15,600 to 26,600 lbs. The total number of IGE and OGE hover conditions was 596. Forward flight test data were obtained at pressure altitudes from sea level to 14,000 feet, and advance ratios from zero to 0.373. The number of forward flight test points was 172. In this paper the wide chord blade data will initially be grouped into three data sets: (1) the combined IGE and OGE hover data, (2) the forward flight data, and (3) the combined hover and forward flight data. Later in the analysis, data from the hover testing will be separated into IGE and OGE categories.

The power measurements obtained on the UH–60L in these tests were the same as used for the Airloads Program. The only difference is that the engine output shaft torquemeters were calibrated in an engine test cell at the U.S. Army's Corpus Christi aircraft overhaul facility rather than using the engine manufacturer's test cell. The aircraft's gross weight was determined in the same way as for the UH–60A Airloads Program. However, for tethered hover testing, the force measured on the tether, using a load cell, was added to the known aircraft weight.

Power Measurement Error Characterization

The total error of a single measurement is comprised of a systematic or constant part of the error, called the bias error, and a stochastic portion, called the precision or repeatability error. Repeated measurements allow an estimate to be made of the precision error, but the bias error is unaffected by replication and can only be identified through calibration. In this paper, the power balance equation, eq. (5), is used as a means of inferring something of the size and type of errors in the power measurements. However, it is not possible from this inference to identify the actual source of measurement errors. Referring to eq. (5), errors in the measurement of the engine output torque, the main rotor torque, and the tail rotor torque each will contribute to the power difference, ΔP, but it is not possible to know which errors are the largest contributors.

The power differences for the four data sets have been calculated using eq. (5) and the basic statistics are summarized in Table 1. If the errors in the power difference equation were precision errors, then the mean value of the power difference would be the unmeasured accessory power, which is estimated to be 66 HP. The deviation from this value for the four data sets ranges from zero to 36 HP. The standard deviation in the power difference varies from 42 to 72 HP while the range varies from 204 to 283 HP. Before assessing the meaning of these statistics it is useful to look at their frequency distribution. Figure 2 shows this frequency distribution

Table 1. – Baseline statistics of power difference, ΔP, for four flight test data sets.

	Mean HP	σ HP	Range HP
Airloads Program	52.3	60.8	228.5
WCB Hover	102.4	71.8	282.6
WCB Level Flight	65.9	42.2	204.3
WCB Combined	94.2	68.1	282.6

for each of the data sets and includes a comparison with a Gaussian or normal distribution. A bin size of 10 HP has been used to determine the experimental data frequency distribution and the data have been normalized by the bin with the largest number of test points. The Gaussian distribution used for comparison has also been normalized to have a value of one. The mean and one standard deviation of the data are indicated on the figure. The accessory power, which is the expected value of the power difference, is shown with an open triangle. This comparison shows that the power differences are not normally distributed, therefore, the mean and standard deviation are not appropriate statistical measures. Furthermore, because the frequency distribution is not normal, there must be other sources of error affecting the data that are not repeatability or precision errors.

Examination of Other Variables

The lack of normality in the power difference distribution in Fig. 2 is evidence that other factors are affecting the power difference. One approach for identifying these unknown factors is to consider other measured parameters as independent variables and use linear regression to determine if there is a relationship between the power difference and the variable. For this examination, eight parameters have been selected: pressure altitude, run number (time), engine output torque, main rotor torque, tail rotor torque, advance ratio, rotor speed, and outside air temperature. For the Airload Program data, pressure altitude was calculated from the density altitude and temperature. The counter or run number is incremented for each test condition and is unique for each flight. This run number is used here as a rough proxy for time. The engine output torque was measured on both engines and was summed. The main rotor torque was measured from a strain-gauge bridge on the main rotor mast and the tail rotor drive shaft torque was taken to be the mean of the two duplicate measurements. Advance ratio, rotor speed, and the outside air temperature were determined using normal flight test measurement procedures. For the WCB Program data, the tabulated powers in Ref. 8 were converted to torque based on the measured main rotor speed. The gear ratio used for the engine output drive shaft was 81.0419 times the main rotor speed and the ratio for the tail rotor drive shaft was 15.958 times the main rotor speed. The remaining tabulated parameters were calculated using normal flight test procedures.

The power difference data for each of the data sets were fit with a first-order linear regression for each of the eight independent variables. One measure of the goodness of fit of a linear regression is the coefficient of determination, r^2 (square of the correlation coefficient). In the examination of a linear regression, the coefficient of determination can be used to estimate how much of the variance in the data set is explained by the independent variable. Thus, if r^2 is one, a perfect fit is achieved and all of the variance is explained by the independent variable. If r^2 is zero, then none of the variance is caused by the independent variable being examined. The r^2 values for the four data sets and the eight independent variables are shown in Table 2. Note that for the wide chord blade hover data set, advance ratio was not considered as an independent variable as it was invariant. Examples of the data and the first-order regression fits are shown in Fig. 3 for the Airloads Program level flight data and in Fig. 4 for the WCB Program combined data. In the majority of cases, the power difference measurement is not related to the independent variable and almost none of the variance is explained. The three exceptions are the pressure altitude (all data sets), run number (WCB Program level flight), and outside air temperature (all data sets). Pressure altitude and temperature are not independent of each other, so it is likely that their influence on the measurement error is a consequence of the same root cause. Temperature accounts for 76% of the variance in the Airloads Program and 43% of the variance in the WCB Program.

Temperature Correction

The effect of the variation of the outside air temperature on the variance in the power difference measurement is substantial. Using the linear regression relation for temperature, it is possible to calculate a power difference with the temperature effects removed

$$\Delta P_T = \Delta P - (a_0 + a_1 T) \qquad (6)$$

where the a_0, and a_1 coefficients were determined from the first-order linear regression fit of ΔP on temperature. Temperature-corrected power differences have been computed for the four data sets and the frequency distributions are examined in Fig. 5. The normality of

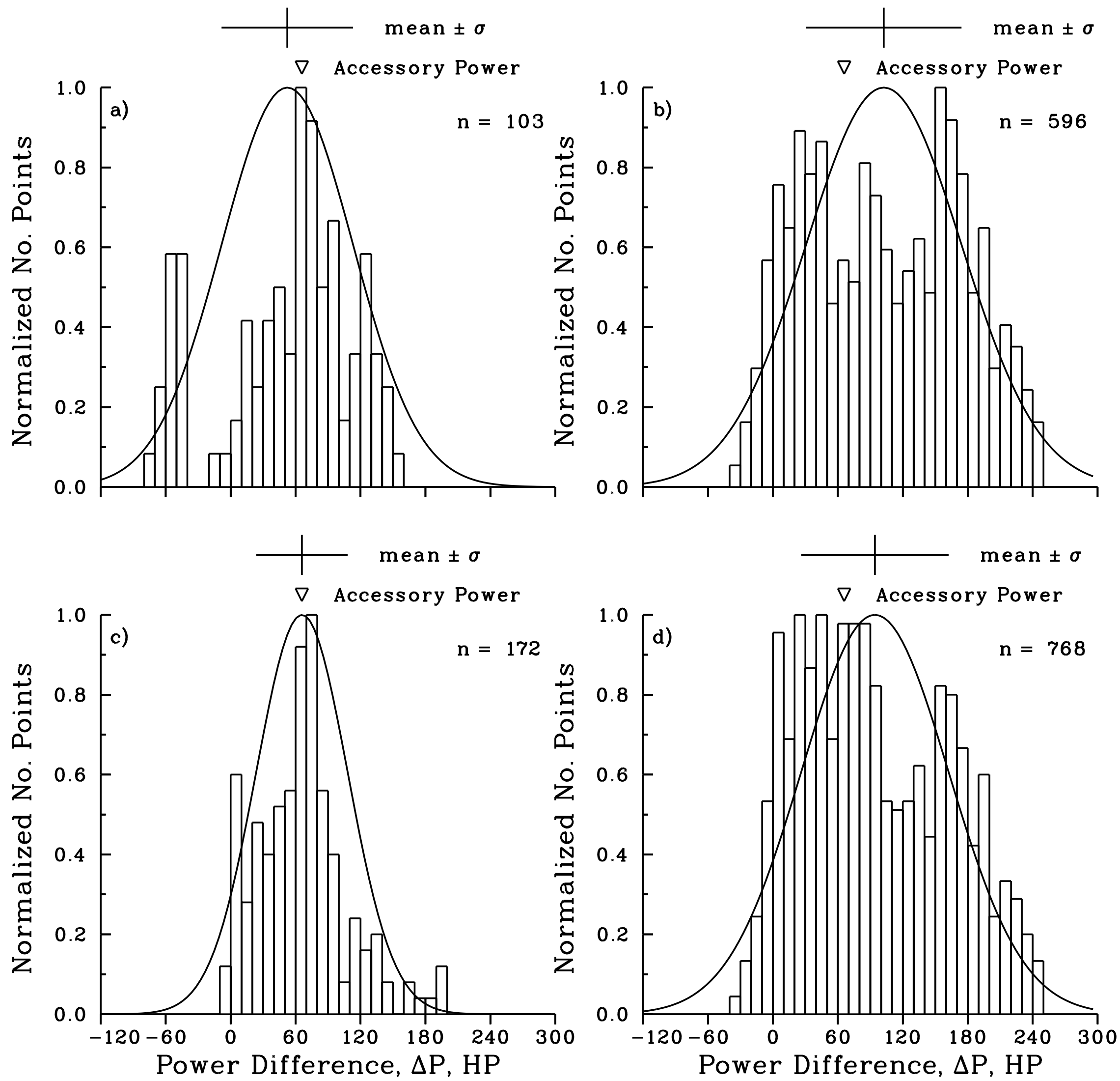

Figure 2. – Frequency distributions of power differences for four data sets: a) Airloads Program level flight data, b) WCB Program hover data, c) WCB Program level flight data, and d) WCB Program combined data.

the distributions is improved over the baseline distributions in Fig. 2, although the variance still appears to be contaminated by extraneous factors. Note that the form of correction used in eq. (6) results in a mean value of zero. The standard deviation and the range for the four data sets are shown in Table 3. The values of the standard deviation are reduced from the baseline case with the Airload Program data set dropping about 51% and the WCB Program data sets dropping 25%. Except for the WCB level flight data set, the range is unaffected.

Examination of Drift

The shift in a measurement over the duration of a flight, that is, between starting and ending zeros, is referred to as drift. The counter number (Airloads Program) or run number (WCB Program) can be used as a proxy for time to look at the effects of drift. The examination of the power difference in Table 2 indicated that the run number had a fairly significant effect (37% of variance) for the WCB Program level flight data set, but did not have a significant effect for the other data sets.

Table 2. – Coefficients of determination, r^2, for power difference as a function of eight variables for the four flight test data sets.

Independent Variable	Airloads Program	WCB Hover	WCB Level Flight	WCB Combined
Pressure altitude	0.63	0.44	0.36	0.43
Run number	0.00	0.02	0.37	0.00
Engine torque	0.03	0.01	0.00	0.02
Main rotor torque	0.09	0.00	0.01	0.00
Tail rotor torque	0.05	0.00	0.06	0.04
Advance ratio	0.00	–	0.02	0.04
Rotor Speed	0.00	0.00	0.01	0.00
Outside air temperature	0.76	0.43	0.43	0.43

Table 3. – Statistics of temperature-corrected power difference for four flight test data sets.

	σ, HP	Range, HP
Airloads Program	29.7	220.2
WCB Hover	54.5	293.9
WCB Level Flight	31.9	153.4
WCB Combined	51.3	294.1

The use of run number as part of the previous linear regression examination was confounded as some test flights included multiple "runs" at different test conditions. For example, Flight 46 (WCB Program level flight) included airspeed sweeps flown at three elevations and hence three different values of outside air temperature. To examine the effects of drift more closely, secondary data sets have been defined that represent subsets of the original data. Each new data set is specified as a single, continuous data run or test run at one operating condition or temperature. For each of these secondary data sets, the run numbers have been shifted so that the first run number is always zero. In addition, the WCB Program hover data have been divided into separate OGE and IGE data sets.

Figure 6 shows the temperature-corrected power difference as a function of the shifted run number for the secondary data sets. The effect of the temperature correction has been to shift the curves closer together, nonetheless, substantial variation remains in these data sets. In the case of the Airloads Program data there is a downward trend in the power difference (negative drift) over the duration of each test run. For the WCB Program OGE and IGE tests, however, the power difference appears to increase over each test run (positive drift). The WCB Program level flight data appear to show a mixture of trends. Oscillations are observed in the WCB Program OGE and IGE hover data and these oscillations appear to correspond to the sequence of torque sweeps at different rotor speeds used in the tethered hover testing.

Neither the cause of the drift in Fig. 6 nor the cause of the offsets between the various test runs are known. Nonetheless, it is possible to fit a first-order linear regression to these data and "correct" for the drift

$$\Delta P_{Td} = \Delta P_T - (a_0 + a_1 N_{run}) \tag{7}$$

where the a_0, and a_1 coefficients are from a first-order linear regression fit of ΔP_T on the shifted run number. The new temperature- and drift-corrected power differences, based on eq. (7), are shown in Fig. 7. These power differences shows reduced variance compared to the temperature-corrected power differences in Fig. 6. The reduced variance is more clearly seen in Fig. 8, which shows the frequency distributions of the temperature- and drift-corrected power differences for the four cases in Fig. 7. The frequency distributions are reasonably normal and the standard deviation and range, as shown in Table 4, are substantially reduced from the previous values in Tables 1 and 3. Note that the data sets that are the basis of the statistical measures in Table 4 are subsets of the previous data sets that were used as a basis for the statistical values in Tables 1 and 3. Thus, the values in Table 4 are only approximately comparable to the previous results.

The reduction in the variance shown here, after correcting for temperature and drift is a highly-idealized situation. In making the initial correction for the outside air temperature there was an implicit assumption that this correction is feasible for flight test measurements if the temperature dependence can be determined from calibration. That a similar calibration approach exists that would allow for the correction of drift is tenuous at best. Nonetheless, the use of an idealized case, as done here, provides an estimate of the accuracy that might be

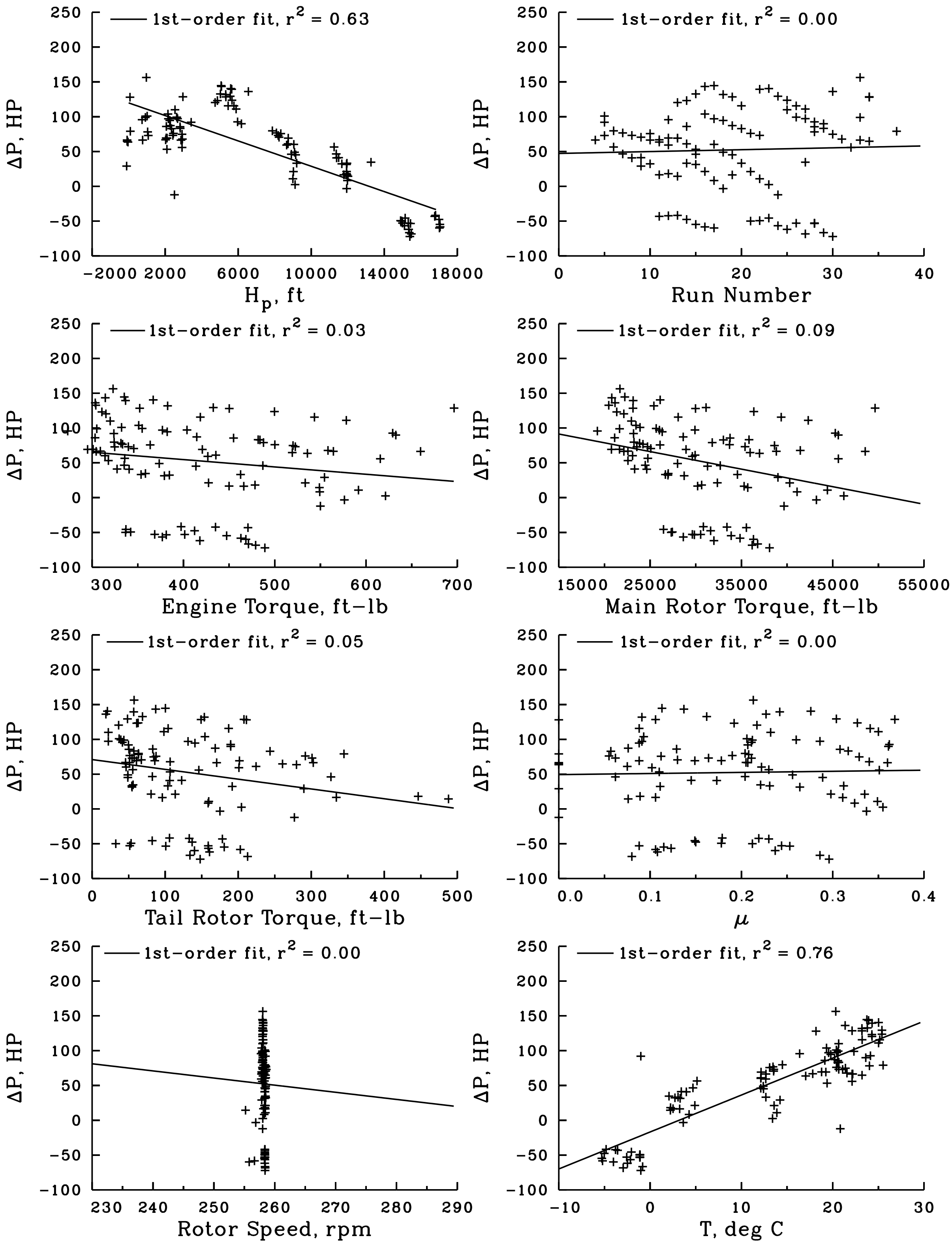

Figure 3. – Power difference dependence on eight parameters; Airload Program level flight data.

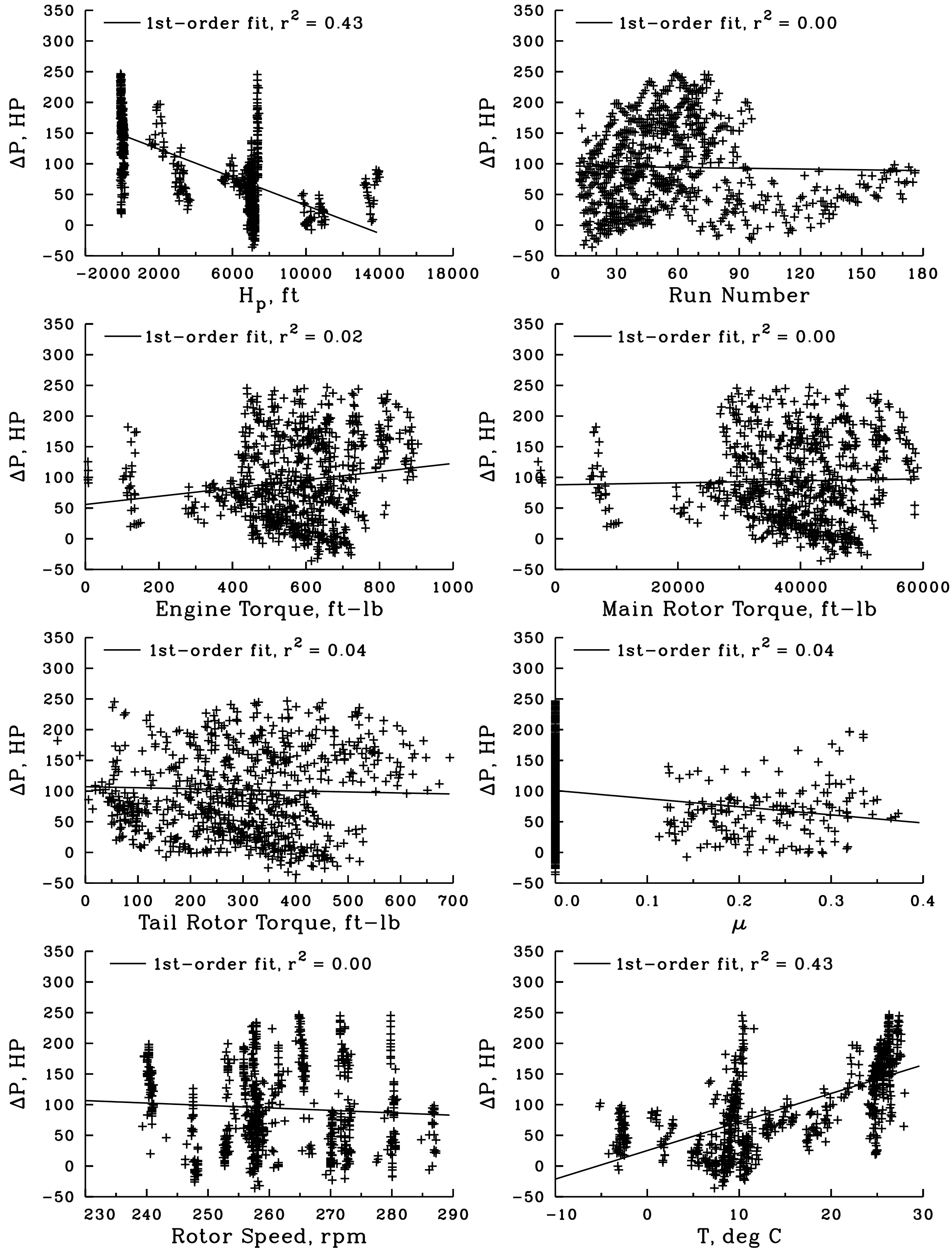

Figure 4. – Power difference dependence on eight parameters; WCB Program combined flight data.

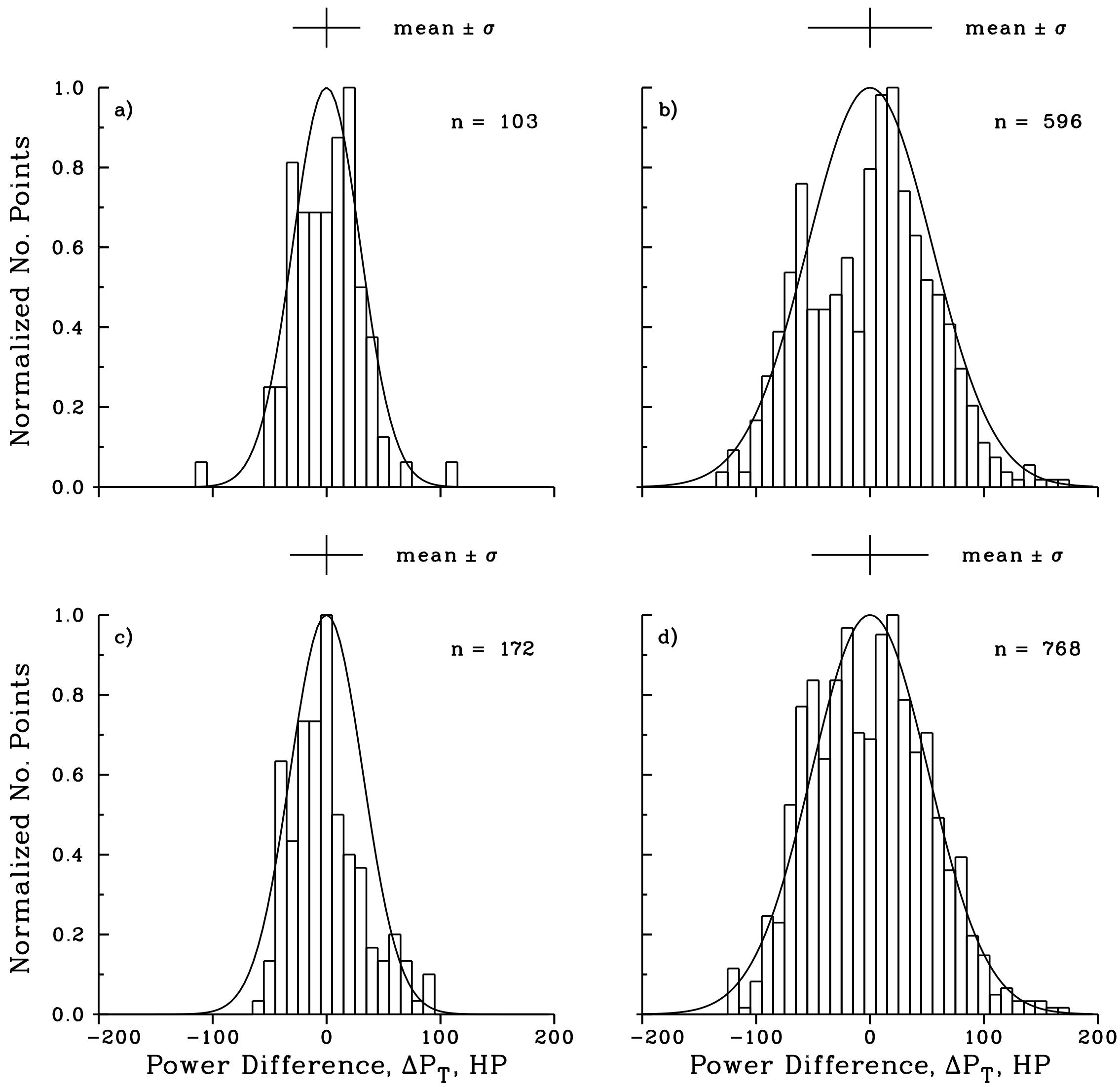

Figure 5. – Frequency distributions of temperature-corrected power differences: a) Airload Program level flight data, b) WCB Program hover data, c) WCB Program level flight data, and d) WCB Program combined data.

Table 4. – Statistics of temperature- and drift-corrected power differences for four flight test data sets.

	σ HP	Range HP
Airloads Program (–)	16.6	139.8
WCB OGE Hover (–)	16.5	78.2
WCB IGE Hover (–)	27.3	159.7
WCB Level Flight (–)	16.9	95.6

achieved if all major measurement problems could be isolated and corrected.

Ambiguity in Experimental Errors

The examination of the power difference has shown that there are substantial errors in power measurements made during performance testing of the UH–60. The use of the power balance equation can demonstrate that these errors are present, but the equation cannot determine the source of the errors. It is possible, however, to examine the various terms in the power balance equation and make a rough assessment of their

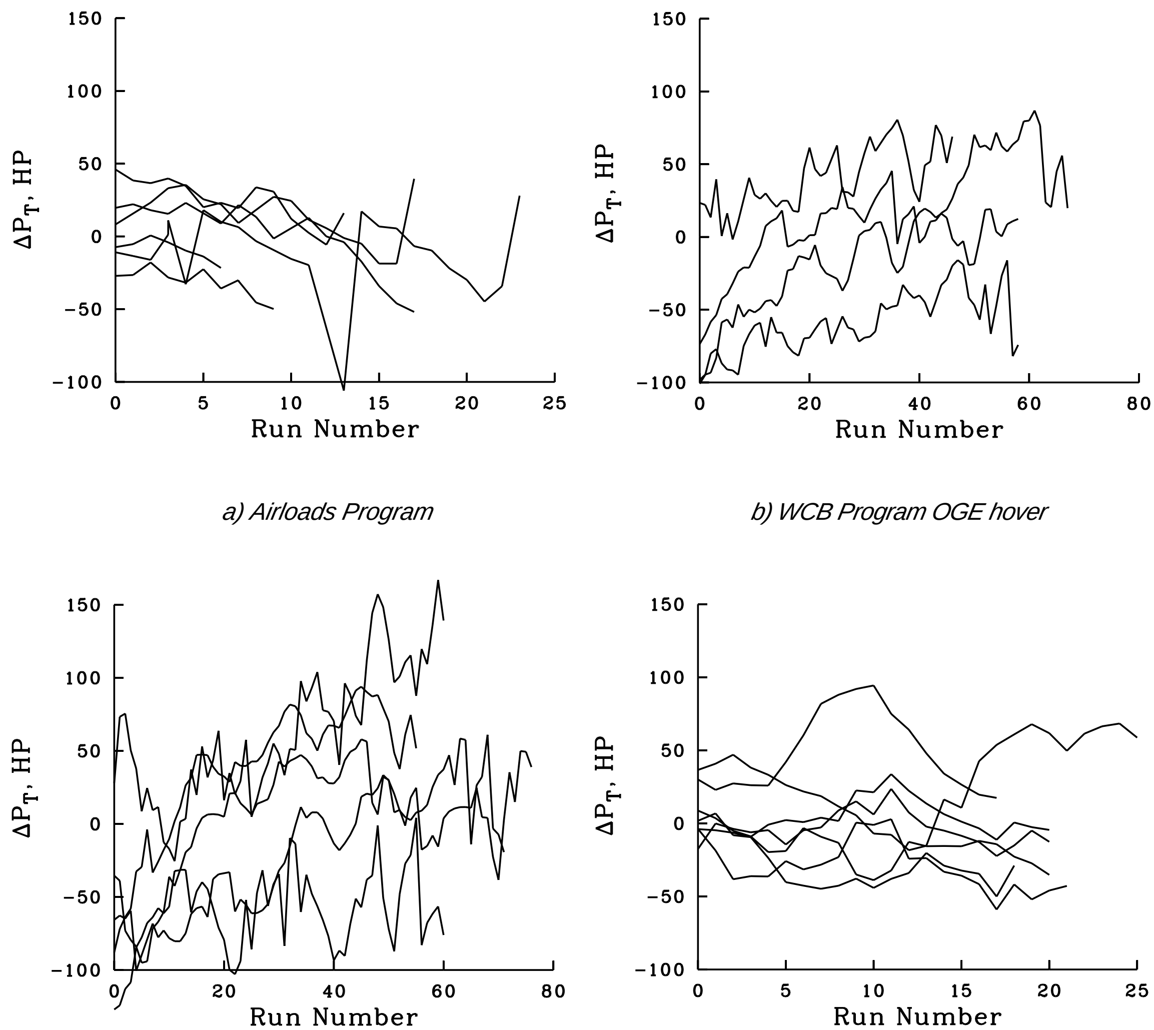

a) Airloads Program

b) WCB Program OGE hover

c) WCB Program IGE hover

d) WCB Program forward flight

Figure 6. – Temperature-corrected power difference as a function of run number.

importance to the power measurement errors. Using all the data in Ref. 8, and normalizing the data such that the main rotor power is 1.00, then the engine output power on this basis is 1.192, the tail rotor power is 0.117, and the unmeasured accessory power is 0.038. Errors of the order of ±5% in either the main rotor power measurements or the engine output shaft power measurement can explain the power measurement errors reported here. Tail rotor and accessory powers, however, are roughly an order of magnitude smaller than the engine and main rotor power, and errors of the size of ±5% cannot explain the power measurement errors. It is likely, therefore, that the errors indicated here are either in the engine torquemeter measurements, the main rotor mast torque measurement, or both.

The UH–60A Operator's Manual, or handbook, is the primary source of performance information for the aircraft and is based on flight test performance data. The performance capability indicated in the handbook is derived from the engine torquemeter measurements rather than main rotor power and, therefore, errors in the main rotor torque measurement will not affect the accuracy of calculations based on the handbook data. However, if errors occur in the engine torquemeter, then the accuracy of handbook calculations will be impacted. Four possible cases can be described where errors are assumed to be in

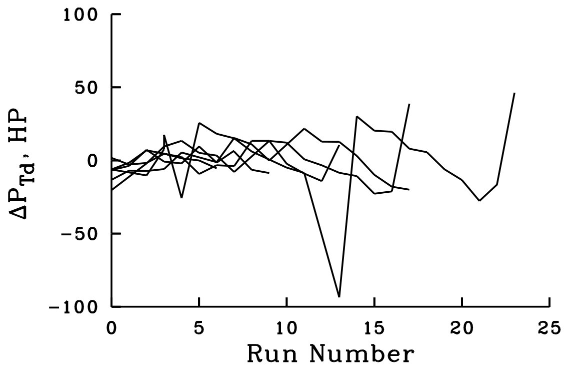

a) Airloads Program

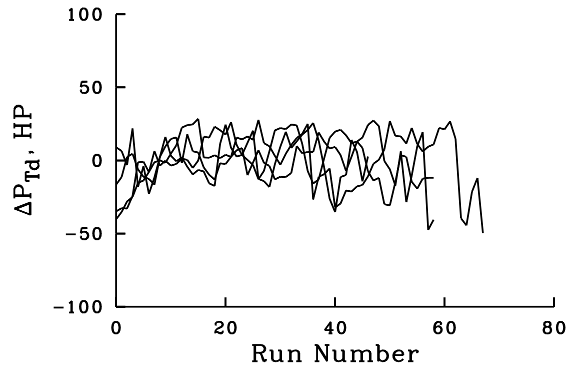

b) WCB Program OGE hover

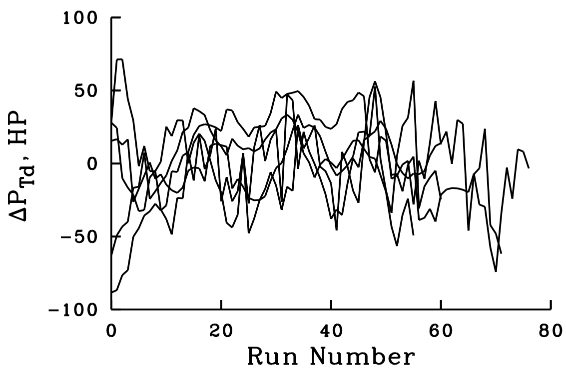

c) WCB Program IGE hover

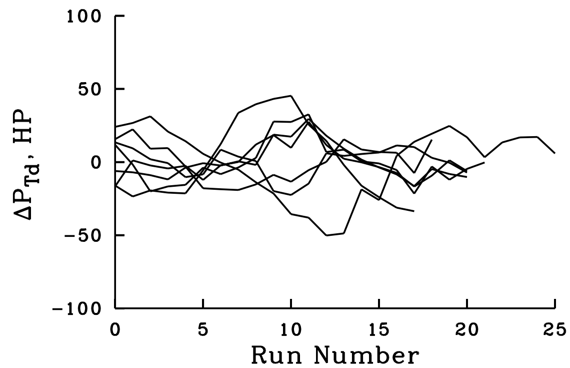

d) WCB Program forward flight

Figure 7. – Temperature- and drift-corrected power differences as a function of run number.

either the engine torquemeter, the main rotor torque measurement, or both. For these purposes, an uncertainty of, roughly, ±125 HP, from Table 1, is used.

Case 1–measurement error in the engine torquemeter. In the case of a –125 HP error the associated handbook data would be optimistic. For a +125 HP error the handbook would be pessimistic.

Case 2–measurement error in the main rotor mast. In this case handbook calculations would be unaffected and the engine torquemeter would provide the correct values.

Case 3–opposite sign errors. If the engine torquemeter has a +75 HP error and the main rotor mast a –50 HP error, then these would add to +125 HP. The handbook would be wrong in this case, but the error would not be as large as in Case 1.

Case 4– same sign errors. If the engine torquemeter error was +300 HP, and the main rotor mast error was +175 HP, then the combined error would be +125 HP. But in this case the handbook data would have larger errors than in Case 1.

The presence of errors is revealed by the examination of the power difference equation, but it is not possible to define the accuracy of the individual power measurements and this situation is unsatisfactory.

Error Sources and Accuracy Requirements

The examination of the power balance equation indicates that there is a temperature dependency in one or more of the power measurements. However, this circumstantial evidence is not sufficient in itself. Although the accuracy of the outside air temperature

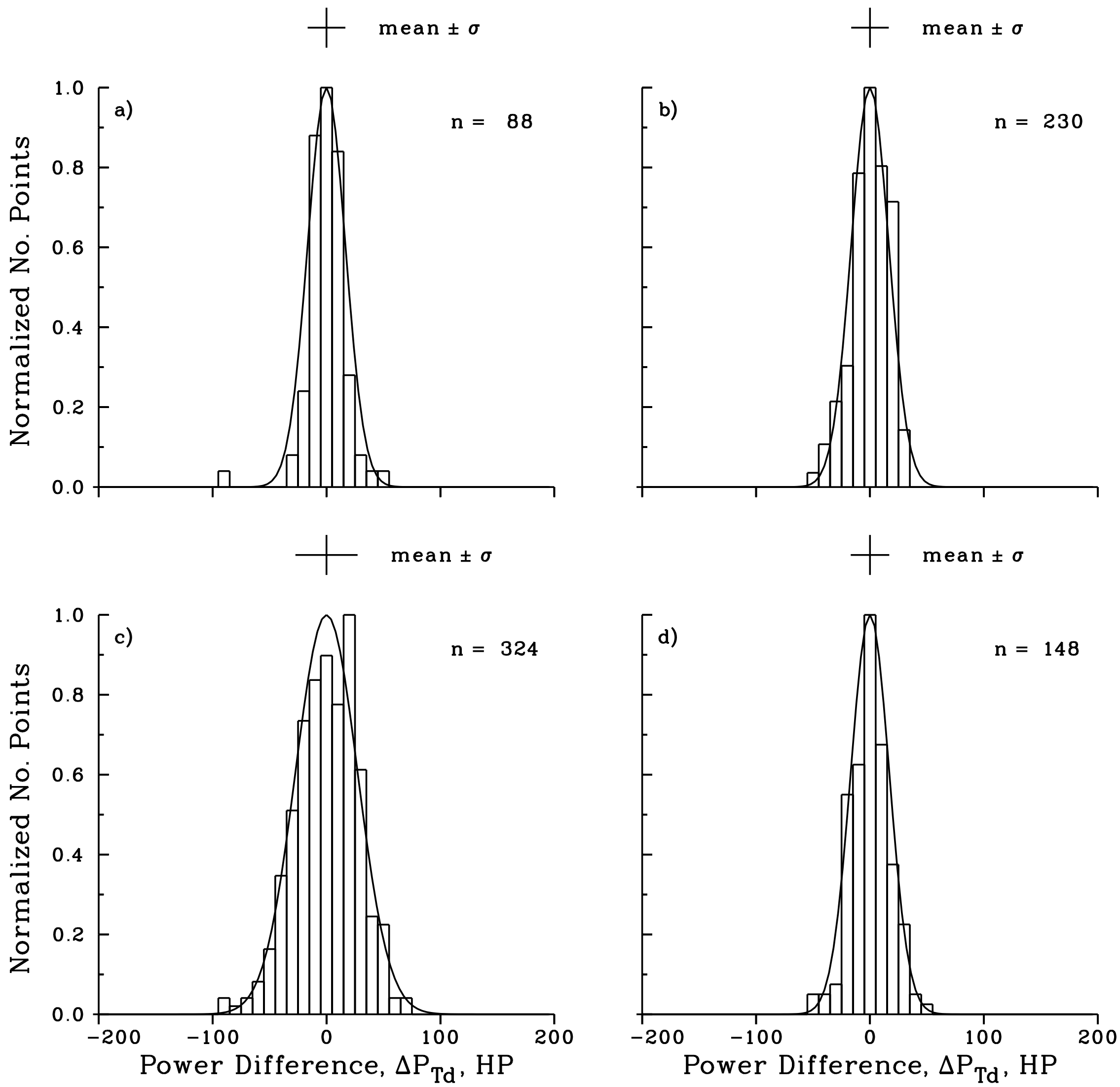

Figure 8. – Frequency distribution of temperature- and drift-corrected power difference: a) Airload Program level flight data, b) WCB Program OGE hover data, c) WCB Program IGE hover data, and d) WCB Program level flight data.

measurement is considered very good, the actual temperatures at the measurement transducer locations are unknown. Moreover, long experience with wind tunnel balance measurements has demonstrated that drift problems in particular are strongly dependent upon both the temperature and the temperature gradients in the vicinity of measurement transducers. In the present situation, neither the temperature at the transducer location nor the gradients are known.

Although the engine torquemeter includes a temperature correction based on exhaust gas temperature, it is not known whether the torquemeter test cell calibrations have ever been performed over a range of ambient temperatures that correspond with those encountered in flight. Similarly, it does not appear that the main rotor mast torque calibration has been performed for variable temperatures either. Without calibrations of this sort it is not possible to determine if appropriate corrections can be made.

This paper has demonstrated that power measurement errors have occurred in UH–60 performance tests. The true size of these errors is unknown as only the sum of the errors can be estimated. Even without knowing the true errors, however, it is useful to consider the measurement accuracy that is required. For this purpose, consider the OGE hover design point for the

UH–60A. The hover performance for this case is shown in Table 5, where the power required is based on the

Table 5. – UH–60A OGE hover design point.

	Value
Gross weight, lbs	16,200
Pressure altitude, ft	4000
Temperature, deg. C	35
Engine power required, HP	2067
Figure of merit	0.615

formulas of Ref. 1. Based on the standard deviation and range from Table 1, the equivalent variation in engine output power, gross weight, and figure of merit have been computed and are shown in Table 6. The power measurement errors represent from ±2.0 to ±5.5% of the engine output power. In terms of gross weight, these errors are equivalent to ±246 to ±666 lbs or roughly one to three combat-equipped troops. The figure of merit is seen to vary from ±1.3 to ±3.4 counts.

The helicopter manufacturer's need for accuracy may be more stringent than that required by the operator. Wake and Baeder (Ref. 11) have stated the manufacturer must achieve a predictive accuracy for hover performance within ±2 counts in figure of merit. Beaumier et al. (Ref. 12) suggest that the accuracy required is ±1.5 counts. A demonstration of such accuracy, of course, requires experimental measurements that are more accurate than the manufacturer's criteria. Such accuracy may be obtainable with careful model-scale experimentation. Based on repeatability measurements, Lorber et al. (Ref. 13) have shown accuracy within ±0.5 counts of figure of merit for a 1/5.73-scale UH–60A model test. Clearly the full-scale measurements reviewed here are not suitable for the validation of analytical models, at least not to the accuracy requirements that have been stated by the manufacturers.

Conclusions

Flight performance measurements from two recent tests of a UH–60 aircraft, performed by different test organizations, have been reviewed. The power balance equation, based on torque measurements of the engine output shaft and the main and tail rotors, has been used to estimate the power measurement errors. Based on this examination, the following conclusions are made.

1. For both flight data sets, errors are observed in the power measurements that are approximately ±5% of the power required. In terms of the aircraft payload these errors are equivalent to one to three combat-equipped troops.
2. The power measurement errors are non-Gaussian and this suggests that unquantified causative factors are affecting these measurements. As the source of these effects are unknown, additional or repeat testing will not reduce these errors.
3. Approximately 45 to 75% of the measurement variance is explained by atmospheric effects, that is, temperature and pressure. Correcting for temperature, using a linear regression fit of the data, reduces the variance in the data and the error distribution becomes more Gaussian.
4. Measurement error is also a result of drift in the power measurements over the course of a test run. It is shown that in an idealized situation, substantial reductions in the power measurement errors may be achieved.

Recommendations

It is recommended that a UH–60 test aircraft be extensively instrumented with temperature transducers to quantify the thermal environment in the region of the engine output shaft torquemeter, the main rotor shaft torsion strain-gauge bridge, and the tail rotor drive shaft torsion bridge. A basic performance testing program should then be undertaken to include tethered hover testing at a minimum of two different site elevations, and forward flight testing at a variety of altitudes and temperatures. Following these flights, the torque measuring devices should be recalibrated to include thermal variation conditions that match those observed in flight. Based on this calibration, the power measurements should be recomputed and power measurement errors reassessed.

Acknowledgments

The author thanks Mr. James O'Malley, US Army Aviation and Missile Command, Huntsville, AL, for his encouragement and support in pursuing this study. Appreciation is expressed to Mr. Frank Dunn, General Electric Company, Lynn, MA, for discussions concerning the design and operation of the T700 engine output shaft torquemeter.

Table 6. – Estimate of accuracy for baseline conditions using minimum and maximum bounds from the four data sets.

	Std. Deviation	Range
Engine output power, HP	±42 to ±72	±102 to ±114
Engine output power, %	±2.0 to ±3.5	±4.9 to ±5.5
Gross weight, lbs	±246 to ±418	±595 to ±666
Figure of merit	±0.013 to ±0.021	±0.030 to ±0.034

References

1. John I. Nagata, Gary L. Skinner, Robert M. Buckanin, Robert D. Robbins, and Robert A. Williams, “Airworthiness and Flight Characteristics Evaluation, UH–60A (Black Hawk) Helicopter,” USAAEFA Project No. 77–17, September 1981.

2. Robert A. Williams, Robert MacMullin, Joseph O. Miess, Robert M. Buckanin, William Abbott, and Gary L. Skinner, “UH–60A External Stores Support System Fixed Provision Fairings Drag Determinations,” USAAEFA Project No. 82–15–1, May 1984.

3. Arthur R. Marshall, Jr., Robert MacMullin, Roy A. Lockwood, Thomas L. Reynolds, Edward J. Tavares, Robert M. Buckanin, Gary L. Skinner, Michael K. Herbst, Charles F. Cassil, Patrick J. Sullivan, and Robert A. Williams, “Airworthiness and Flight Characteristics Test of a Sixth Year Production UH–60A,” USAAEFA Project No. 83–24, June 1985.

4. Robert A. Williams, Gary L. Skinner, Robert MacMullin, Robert M. Buckanin, Joseph C. Miess, Michael K. Herbst, and Edward J. Tavares, “UH–60A Expanded Gross Weight and Center of Gravity Evaluation,” USAAEFA Project No. 81–16, August 1985.

5. Robert M. Buckanin, Warren Gould, Paul W. Losier, David A. Downey, Roy Lockwood, James L. Webre, John F. Hagen, Randall W. Cason, and Christopher J. Young, “Rotor System Evaluation, Phase I,” AEFA Project No. 85–15, March 1988.

6. John I. Nagata, Joseph L. Piotrowski, Christopher J. Young, William D. Lewis, Paul W. Losier, and Joseph A. Lyle, “Baseline Performance Verification of the 12th Year Production UH–60A Black Hawk Helicopter,” USAAEFA Project No. 87–32, January 1989.

7. Kufeld, R. M., Balough, D. L., Cross, J. L., Studebaker, K. F., Jennison, C. D., and Bousman, W. G., “Flight Testing the UH–60A Airloads Aircraft,” American Helicopter Society 50th Annual Forum Proceedings, Washington, D.C., May 11-13, 1994, pp. 557–578.

8. Boirun, B., and Ludlam, J., “H–60 Growth Rotor Blade (GBR) Performance and Powerplants Qualification Flight Test Report,” SER-702639, January 2000.

9. David T. Balch, “Experimental Study of Main Rotor/Tail Rotor/Airframe Interaction in Hover,” *Journal of the American Helicopter Society*, Vol. 30, (2), April 1985, pp. 49–56.

10. William G. Bousman, “Discrepancies in the Measurement of Aircraft and Rotor Power,” Occasional Note 1999-04, March 1999, http://rotorcraft.arc.nasa.gov/research/pdfs/1999-04.pdf.

11. Brian E. Wake and James D. Baeder, “Evaluation of a Navier-Stokes Analysis Method for Hover Performance Prediction,” *Journal of the American Helicopter Society*, Vol. 41, (1), January 1996, pp. 7–17.

12. P. Beaumier, C. Castellin, and G. Arnaud, “Performance Prediction and Flowfield Analysis of Rotors in Hover, Using a Coupled Euler/Boundary Layer Method,” Paper No. AE12, 24th European Rotorcraft Forum, Marseilles, France, September 15-17, 1998.

13. Peter F. Lorber, R. Charles Stauter, Michael J. Pollack, and Anton J. Landgrebe, “A Comprehensive Hover Test of the Airloads and Airflow of an Extensively Instrumented Model Helicopter Rotor; Volume 1 – Rotor Airloads and Performance,” USAAVSCOM TR 91-D-16A, October 1991.